





## Fragmentation of the ${}^4\text{He}_2$ dimer by relativistic highly charged projectiles in collisions with small kinetic energy release

B. Najjari <sup>1,\*</sup>, S. F. Zhang <sup>1</sup>, X. Ma <sup>1</sup> and A. B. Voitkiv <sup>2,†</sup>

<sup>1</sup>*Institute of Modern Physics, Chinese Academy of Sciences, Lanzhou 730000, China*

<sup>2</sup>*Institute for Theoretical Physics I, Heinrich-Heine-Universität Düsseldorf, Universitätsstrasse 1, 40225 Düsseldorf, Germany*



(Received 11 April 2022; accepted 26 May 2022; published 9 June 2022)

We study theoretically the fragmentation of the helium dimer,  ${}^4\text{He}_2$ , into singly charged ions in collisions with relativistic highly charged projectiles. We discuss the main mechanisms driving this process with the focus on the fragmentation caused by direct ionization of both atomic sites of the dimer in a single collision with the projectile. This direct mechanism dominates the  $\text{He}_2 \rightarrow \text{He}^+ + \text{He}^+$  breakup events with the kinetic energies of the emerging ionic fragments below 4–5 eV. We explore the energy and angular distributions of the  $\text{He}^+$  ions produced in collisions with 1 and 7 GeV/u  $\text{U}^{92+}$  projectiles and show that their shape is significantly affected by relativistic and higher-order effects in the interaction between the projectile and the dimer. We also show that the shape of the energy spectrum is quite sensitive to the binding energy of the  $\text{He}_2$  dimer, which can be exploited for its precise determination. The contribution of the direct mechanism to the total cross section for the  $\text{He}_2$  fragmentation by 1 and 7 GeV/u  $\text{U}^{92+}$  was calculated to be 3.65 Mb and 2.4 Mb, respectively, representing roughly half of this cross section.

DOI: [10.1103/PhysRevA.105.062807](https://doi.org/10.1103/PhysRevA.105.062807)

### I. INTRODUCTION

The study of fast ion-atom and ion-molecule collisions already has a long history. However, collisions of fast ions with very extended atomic objects, like humongous van der Waals dimers, are very rarely considered, even though compared to the “normal” case the physics of such collisions possesses new and interesting features.

In particular, to our knowledge there are just a few papers [1–5] where collisions of fast ions with the  $\text{He}_2$  and Li-He dimers were studied. In [1–3] and [5] the fragmentation process  $\text{He}_2 \rightarrow 2 \text{He}^+ + 2 e^-$  was explored for collisions with different projectiles and at different impact velocities while in [4] single ionization of the Li-He dimer by ultrafast projectiles involving energy transfer between the dimer atoms was considered.

Both the  $\text{He}_2$  and Li-He dimers are spectacular pure quantum systems. For instance, in the  $\text{He}_2$  dimer the interaction between two ground-state helium atoms is so weak that it supports one bound state only, which has an extremely small binding energy ( $\simeq 10^{-7}$  eV, [6]). The size of this two-atomic bound system is enormous: its average bond length is  $\approx 50$  Å [6] and the dimer extends to the distances of more than 200 Å, that makes it the largest known ground-state diatomic molecule. The outer classical turning point in the ground state of the dimer is about 14 Å [7], which is almost four times smaller than its average bond length, showing that the  $\text{He}_2$  dimer is a quantum halo system which spends most of the time in the classically forbidden region. Because of its enormous size the interatomic interaction and the dimer binding energy

are noticeably influenced by the Casimir-Polder retardation effect [8,9].

When the  $\text{He}_2$  interacts with external electromagnetic fields a multitude of various processes becomes possible. They include a fragmentation of the  $\text{He}_2$  dimer into helium ions, which may occur when the dimer is irradiated by an electromagnetic wave or bombarded by charged projectiles. Helium ions repeal each other that results in a Coulomb explosion of the system. The kinetic energy of the ionic fragments, which is released in this explosion, depends on their charges and the initial distance between them. The spectra of the kinetic energy release may contain valuable information about the structure of the initial  $\text{He}_2$  dimer as well as transient dimers (which may be formed if the time interval between the interaction with the external field and the start of the Coulomb explosion is sufficiently large). Some of these fragmentation processes were already studied.

The fragmentation of the  $\text{He}_2$  dimer into  $\text{He}^+$  ions, caused by the absorption of a single photon, was considered in [10–12]. In [13] the process of  $\text{He}_2$  fragmentation into  $\text{He}^+$  ions, induced by absorption of two high-frequency photons, was employed to sample the dimer wave function at interatomic distances  $R \gtrsim 10$  Å, which enabled the authors to accurately measure the binding energy of the dimer.

The process of  $\text{He}_2$  fragmentation into singly charged ions in collisions with 150 keV/u alpha particles and 11.37 MeV/u  $\text{S}^{14+}$  projectiles was explored in [1] and [2,3], respectively, where the focus was on the fragmentation events with kinetic energies of the  $\text{He}^+$  ions greatly exceeding 1 eV.

Very recently, the process of  $\text{He}_2$  fragmentation in collisions with relativistic highly charged projectiles was considered in [5]. Unlike [1–3], in [5] the fragmentation events with kinetic energies of  $\text{He}^+$  ions not significantly exceeding 1 eV were explored. In particular, it was shown in [5] that

\*b.najjari@impcas.ac.cn

†alexander.voitkiv@tp1.uni-duesseldorf.de

the lower-energy part of the fragmentation spectrum can be very strongly influenced by relativistic effects caused by the collision velocity approaching the speed of light and that the calculated energy spectrum is quite sensitive to the value of the dimer binding energy, which can be exploited for measuring this energy.

In the present paper we continue to study the fragmentation reaction  $\text{He}_2 \rightarrow 2 \text{He}^+ + 2 e^-$  in relativistic collisions with highly charged ions. Like in [5], we will focus here on the fragmentation mechanism in which the projectile directly ionizes both helium atoms in a single collision. At relativistic collision velocities this mechanism becomes very long-ranged and, therefore, is especially suited to probe the ground state of the  $\text{He}_2$  at interatomic distances  $R \gtrsim 10$  a.u., where it already completely dominates the fragmentation process.

The paper is organized as follows. The next section begins with a discussion of the main fragmentation mechanisms which are present in collisions with relativistic highly charged ions. Then we consider a theoretical description of the direct fragmentation mechanism mentioned above. In Sec. III we present our results for the fragmentation cross sections. Section IV contains the main conclusions.

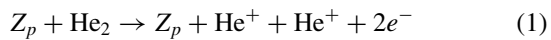
Atomic units ( $\hbar = |e| = m_e = 1$ ) are used throughout unless otherwise stated.

## II. GENERAL CONSIDERATION

### A. Main fragmentation mechanisms

Let the  $\text{He}_2$  dimer collide with a projectile, which has a charge  $Z_p$  and moves with a velocity  $v$  whose magnitude approaches the speed of light  $c \approx 137$  a.u. At  $v \sim c$  the parameter  $\eta = Z_p/v$ , characterizing the effective strength of the projectile field in the collision, is well below 1, which indicates that the field of the projectile in the collision is weak overall rather than strong. Consequently, the breakup of the  $\text{He}_2$  will occur with a nonnegligible probability only provided the number of “steps” in the interaction of the projectile with the constituents of the dimer is reduced to a necessary minimum. Also, in relativistic collisions with very light atoms, the processes of radiative and nonradiative electron capture from the atom by the projectile are already extremely weak, having cross sections which are by several orders of magnitude smaller than atomic ionization and excitation cross sections [14–17].

The above features inherent to high-energy collisions with light targets restrict the number of the main fragmentation mechanisms, which govern the breakup of the  $\text{He}_2$  dimer into  $\text{He}^+$  ions



by high-energy charged projectiles, to four [5].

#### 1. Mechanisms of the “delayed” fragmentation

Two of these mechanisms can be termed as “delayed” since the average time, which they require for the formation of the  $\text{He}^+-\text{He}^+$  system, is determined by the motion of the helium nuclei and, therefore, exceeds by several orders of magnitude the time, which is needed by the projectile to traverse the region of space occupied by the initial  $\text{He}_2$  dimer. These

mechanisms are also characterized by relatively large values of the kinetic energy of the  $\text{He}^+$  fragments. Both of them involve the interaction between the projectile and just one site of the  $\text{He}_2$  dimer.

(i) In the first of these mechanisms the collision between the projectile and one of the helium atoms results in its double ionization. Then the  $\text{He}^{2+}-\text{He}$  system evolves until the  $\text{He}^{2+}$  radiatively captures one electron from the neutral helium atom and the resulting  $\text{He}^+-\text{He}^+$  system undergoes a Coulomb explosion. According to its steps, this mechanism can be denoted as double-ionization–radiative-electron-transfer (DI-RET).

The fragmentation cross section  $\sigma_{\text{fr}}^{\text{DI-RET}}$  for this mechanism can be evaluated as  $\sigma_{\text{fr}}^{\text{DI-RET}} = 2 \sigma_{\text{He}}^{2+} P_{\text{RET}}$ , where  $\sigma_{\text{He}}^{2+}$  is the cross section for double ionization of the helium atom by the projectile and  $P_{\text{RET}}$  the probability for radiative electron transfer. In relativistic collisions with very highly charged projectiles ( $Z_p \sim v$ ) the cross section  $\sigma_{\text{He}}^{2+}$  reaches several tens of megabarns which in turn results in the magnitude of the  $\sigma_{\text{fr}}^{\text{DI-RET}}$  of the order of megabarn (see Sec. III D).

Within the reflection approximation, the kinetic energy  $E_K$  of the ionic fragments, which is released in a Coulomb explosion, is related to the internuclear distance  $R$  at which the explosion started: in particular, for singly charged ions one has  $E_K = 1/R$ . The experimental results of [13] and the theoretical consideration of [18] show that in the case of  $\text{He}_2$  the reflection approximation is quite accurate up to very low energies ( $E_K \sim 1$  meV) where it starts to be violated by the recoil effects.

Since radiative electron transfer occurs only at small internuclear distances (not exceeding a few atomic units) the DI-RET mechanism leads to fragmentation with relatively large kinetic energy release: the results of [1] and [3] show that, in collisions with fast charged projectiles, the energy spectrum of the fragments, which are produced via this mechanism, peaks at  $E_K \approx 9$  eV corresponding to  $R \approx 3$  a.u. and that its intensity rapidly decreases when the energy  $E_K$  departs from this value.

(ii) In the second “delayed” fragmentation mechanism the projectile also interacts with just one helium atom. Now, however, the interaction results in simultaneous ionization–excitation of this atom. In the presence of a neutral helium atom the excited helium ion can de-excite not only via spontaneous radiative decay, but also by transferring energy to the neutral He atom that leads to ionization of the latter.

Such an energy transfer acquires a relatively large effective range becoming quite efficient if the  $\text{He}^+$  ion is produced in an excited state which can decay to the ground state by an electric dipole transition. Then the energy transfer occurs mainly via dipole-dipole two-center electron transitions.

To our knowledge, a radiationless relaxation of an excited atom via energy transfer to a neighbor atom, which at large interatomic distances occurs predominantly via the dipole-dipole interaction, was first considered theoretically in [19]. In the process, which was studied in [19] and termed there the *interatomic Auger decay* (IAAD), the excited atom initially has a vacancy which is filled by its electron, but, unlike in “normal” (intraatomic) Auger decay the energy release is transferred to the neighbor atom ionizing it. The process of IAAD was shown in [19] to be so efficient that it can even outperform intraatomic Auger decay.

Based on the dipole-dipole approximation for the interaction between two atoms at large interatomic distances, in [19] also a simple approximate formula was derived for the IAAD rate  $\Gamma_a$ . Being adapted to the case under consideration, the formula reads

$$\Gamma_a = \alpha \left(\frac{c}{\omega}\right)^4 \frac{\Gamma_r \sigma_{\text{ph}}^{\text{He}}(\omega)}{R^6}. \quad (2)$$

Here,  $\alpha$  is a numerical constant dependent on the excited state of the  $\text{He}^+$  ion [20],  $\Gamma_r$  is the rate for spontaneous radiative decay of the excited state of the  $\text{He}^+$  ion,  $\omega$  is the energy difference between the excited and ground states of the  $\text{He}^+$  ion which is transferred to the He atom,  $\sigma_{\text{ph}}^{\text{He}}(\omega)$  is the cross section for single ionization of the He atom by absorption of a photon with frequency  $\omega$ ,  $R$  is the distance between the  $\text{He}^+$  and He, and  $\alpha$  is a numerical parameter  $\sim 1$  depending on the magnetic quantum number of the excited state of the  $\text{He}^+$ .

The process of IAAD in a system of two atomic particles, where relaxation via intraatomic Auger decay is not allowed energetically, was computed in [21] and was called there the *interatomic coulombic decay* (ICD). Nowadays the term ICD is often understood more generally and used to denote all interatomic/intermolecular radiationless relaxation mechanisms, in which an overlap between electronic shells of the interacting particles is not required since the energy is transferred via the exchange of virtual photons between them. Accordingly, the fragmentation mechanism, in which simultaneous ionization-excitation of one of the atoms by the projectiles is followed by ICD decay, can be denoted as IE-ICD.

The process of ICD in the  $\text{He}^+ - \text{He}$  system competes with spontaneous radiative decay, which does not result in the production of the second helium ion. Using Eq. (2) and assuming for definiteness that the excited  $\text{He}^+$  ion was produced in a  $2p$  state we obtain for the ratio  $\Gamma_a/\Gamma_r \approx \beta (10/R)^6$ , where  $\beta \sim 1$ . This indicates that when the distance  $R$  between the  $\text{He}^+$  and He significantly exceeds 10 a.u. the ICD channel becomes inefficient (in the experiment [11] on the  $\text{He}_2$  photo fragmentation the ICD was clearly “visible” up to  $R \approx 12$  a.u.). According to the results of [1] and [3] in fast collisions with charged projectiles the IE-ICD is very efficient in producing  $\text{He}^+$  ions with energies in the vicinity of  $E_K \approx 8$  eV, but is, in essence, completely inactivated above 10 eV and below 4 eV. As rough estimates suggest (see Sec. III D), in relativistic collisions with very highly charged projectile the sum of the contributions  $\sigma_{\text{fr}}^{\text{IE-ICD}}$  and  $\sigma_{\text{fr}}^{\text{DI-RET}}$  to the total fragmentation cross section may reach a few megabarns.

(iii) The average size of the  $\text{He}_2$  dimer greatly exceeds not only the effective range of RET, but also that of ICD. Therefore, there must occur a very significant contraction of the intermediate  $(\text{He}^+)^* - \text{He}$  and  $\text{He}^{2+} - \text{He}$  dimers before the distance between the nuclei sufficiently decreases in order for the ICD and RET to come into the play. The contraction is possible because the potential of the  $\text{He}^{2+} - \text{He}$  and  $(\text{He}^+)^* - \text{He}$  systems at large internuclear distances is attractive.

## 2. Mechanisms of the “instantaneous” fragmentation

In collisions with high-energy projectiles there are two more fragmentation mechanisms in which, unlike

the DI-RET and IE-ICD, the  $\text{He}^+ - \text{He}^+$  system emerges “instantaneously,” i.e., on the so short timescale that, during the production of two helium ions, the helium nuclei remain essentially at rest.

(i) In one of them the projectile interacts with both atoms of the dimer. As a result, each helium atom emits an electron and becomes a singly charged ion. In this fragmentation mechanism the projectile directly forms the  $\text{He}^+ - \text{He}^+$  system [22] which undergoes a Coulomb explosion. Since the size of the  $\text{He}_2$  is very large, the interactions between the constituents of the dimer play in this mechanism no noticeable role. In [5] this mechanism was termed *the direct fragmentation* (DF) and we shall use it also here.

We note that at relativistic impact velocities the time interval  $T$  between the collisions of the projectile with the first and second atoms of the  $\text{He}_2$  dimer does not exceed a few atomic units ( $T \lesssim 10^{-16}$  s). This is by orders of magnitude smaller than typical nuclear times ( $\sim 10^{-13} - 10^{-12}$  s) in the  $\text{He}^+ - \text{He}$  system, showing that the DF mechanism is indeed “instantaneous.”

(ii) In the other “instantaneous” fragmentation mechanism the projectile interacts with just one atom of the dimer. As a result of this interaction, the atom emits an electron. There is a certain probability that the emitted electron will move towards the other atom and knock out one of its electrons. Thus, this fragmentation mechanism is a combination of single ionization of the helium atom by a high-energy projectile and the so-called *e-2e* process on helium (single ionization by electron impact). Following [5] we shall refer to this mechanism as *single ionization-e-2e* (SI-e-2e) [23].

In the SI-e-2e process the velocity of the first emitted electron is by two orders of magnitude smaller than the velocity of the relativistic projectile. Nevertheless, this electron still moves much faster than the helium nuclei. With its typical velocity  $v_e \sim 1$  a.u., we obtain that the time, which the electron needs to propagate between the sites of the dimer, does not exceed  $10^{-14}$  s. Since this time is much shorter than typical nuclear times in the  $\text{He}^+ - \text{He}$  system, the SI-e-2e mechanism can be also viewed as “instantaneous.”

Since in both the DF and SI-e-2e the helium ions emerge at “frozen” positions of the helium nuclei, their energy  $E_K$  is very simply ( $E_K = 1/R$ ) related to the size  $R$  of the  $\text{He}_2$  dimer at the collision instant (as long as the recoil effects can be ignored, see Sec. II B).

The cross section for the production of two singly charged helium ions by relativistic projectiles via the DF mechanism depends on the transverse size  $R_\perp$  of the  $\text{He}_2$  dimer [5], scaling approximately as  $1/R_\perp^2$ . The corresponding cross section for the production via the SI-e-2e depends on the dimer size  $R$  as  $1/R^2$  [5].

Thus, unlike the DI-RET and IE-ICD, the DF and SI-e-2e mechanisms are not only instantaneous, providing a simple correspondence between the kinetic energy release and the size of the  $\text{He}_2$  dimer, but also possess much longer effective range. Therefore, they are especially suited for probing the ground state of the  $\text{He}_2$  in a very large interval of the interatomic distances  $R$ .

It was shown in [5] that in collisions of  $\text{He}_2$  dimers with very highly charged projectiles ( $Z_p/v \sim 1$ ) the DF mechanism is much more efficient than the SI-e-2e yielding cross sections

which are larger by orders of magnitude. Therefore, in the rest of the paper we shall concentrate on the He<sub>2</sub> fragmentation via the DF mechanism.

### B. Direct fragmentation mechanism

We shall consider collisions between the He<sub>2</sub> dimer and the projectile using the semi-classical approximation in which the relative motion of the heavy particles (nuclei) is treated classically whereas the electrons are considered quantum mechanically.

We choose a reference frame in which the dimer is at rest and take the nucleus of one of its atoms as the origin. We shall refer to this atom as atom *A* whereas the other will be denoted by *B*. In this frame, the coordinates of the nucleus of atom *B* are given by the internuclear vector  $\mathbf{R}$  of the dimer and the projectile moves along a classical straight-line trajectory  $\mathbf{R}_p(t) = \mathbf{b} + \mathbf{v}t$ , where  $\mathbf{b} = (b_x, b_y, 0)$  is the impact parameter with respect to the nucleus of atom *A* and  $\mathbf{v} = (0, 0, v)$  the collision velocity.

Since the size of the He<sub>2</sub> dimer is very large, the ionization of atoms *A* and *B* occurs independently of each other and we can use the independent electron approximation. According to it the probability  $P_{A+B^+}$  for single ionization of atoms *A* and *B* in the collision where the projectile moves with an impact parameter  $\mathbf{b}$  is given by

$$P_{A+B^+} = P_{A^+}(\mathbf{b})P_{B^+}(\mathbf{b}'). \quad (3)$$

Here,  $P_{A^+}(\mathbf{b})$  and  $P_{B^+}(\mathbf{b}')$  are the probabilities for the single ionization of atoms *A* and *B*, respectively, and  $\mathbf{b}' = \mathbf{b} - \mathbf{R}_\perp$  is the collision impact parameter with respect to atom *B*, where  $\mathbf{R}_\perp$  is the part of the internuclear vector  $\mathbf{R}$  of the dimer which is perpendicular to the projectile velocity  $\mathbf{v}$ .

Within the independent electron approximation the probabilities for single ionization of helium atoms *A* and *B* read

$$\begin{aligned} P_{A^+}(\mathbf{b}) &= 2w(\mathbf{b})[1 - w(\mathbf{b})], \\ P_{B^+}(\mathbf{b}') &= 2w(\mathbf{b}')[1 - w(\mathbf{b}')], \end{aligned} \quad (4)$$

where  $w(\mathbf{b})$  [ $w(\mathbf{b}')$ ] is the probability to remove one electron from the helium atom in the collision with a projectile having an impact parameter  $\mathbf{b}$  ( $\mathbf{b}'$ ) [24].

The quantity

$$\begin{aligned} \sigma_{A+B^+}^{\text{DF}} &= \int d^2\mathbf{b} P_{A+B^+}(\mathbf{b}) \\ &= \int d^2\mathbf{b} P_{A^+}(\mathbf{b}) P_{B^+}(\mathbf{b}') \\ &= \int d^2\mathbf{b} P_{A^+}(\mathbf{b}) P_{B^+}(\mathbf{b} - \mathbf{R}_\perp) \end{aligned} \quad (5)$$

represents the cross section for the production of two singly charged helium atom by the projectile in the collision with the He<sub>2</sub> dimer at a given internuclear vector  $\mathbf{R}$  of the latter. Since the probabilities  $P_{A^+}(\mathbf{b})$  and  $P_{B^+}(\mathbf{b}')$  depend just on the absolute value of the respective impact parameters,  $P_{A^+}(\mathbf{b}) \equiv P_{A^+}(b)$  and  $P_{B^+}(\mathbf{b}') \equiv P_{B^+}(b')$ , the cross section (5) depends only on the absolute value  $R_\perp$  of the two-dimensional vector  $\mathbf{R}_\perp$ :  $\sigma_{A+B^+}^{\text{DF}} = \sigma_{A+B^+}^{\text{DF}}(R_\perp)$ .

In our calculations of the probabilities  $w(b)$  and  $w(b')$  we regard the helium atom in its initial and final states as an

effectively single-electron system, where the ‘‘active’’ electron moves in the effective field, created by the ‘‘frozen’’ atomic core consisting of the atomic nucleus and the ‘‘passive’’ electron. This field is approximated by the potential

$$V(\mathbf{r}) = -\frac{1}{r} - (1 + \beta r) \frac{\exp(-\alpha r)}{r},$$

where  $r$  is the distance between the active electron and the atomic nucleus and  $\alpha = 3.36$  and  $\beta = 1.665$  [25]. We note that with this choice of  $\alpha$  and  $\beta$ ,  $V(\mathbf{r})$  almost coincides with the exact Hartree-Fock potential.

The cross section (5) can be only computed numerically and the computation is quite time consuming. However, a simple estimate can be obtained for this cross section at  $R_\perp \gg 1$  a.u. [5]

$$\sigma^{\text{DF}} \approx C \frac{Z_p^4}{v^4 \gamma^2} \left[ K_1^2\left(\frac{R_\perp}{R_a}\right) + \frac{1}{\gamma^2} K_0^2\left(\frac{R_\perp}{R_a}\right) \right]. \quad (6)$$

Here,  $K_0$  and  $K_1$  are the modified Bessel function [26],  $R_a = \frac{\gamma v}{\bar{\omega}}$  is the adiabatic collision radius, where  $\gamma = 1/\sqrt{1 - v^2/c^2}$  is the collision Lorentz factor,  $\bar{\omega} \approx 1.2$  a.u. is the mean transition frequency for single ionization of a helium atom, and  $C$  is a free (fit) parameter which is a very slowly varying function of  $R_\perp$  [27].

Taking into account that  $K_0(x) \sim \ln(1.12/x)$  and  $K_1(x) \sim 1/x$  if  $x < 1$  whereas  $K_0(x) \sim K_1(x) \sim \sqrt{\frac{\pi}{2x}} \exp(-x)$  at  $x > 1$ , it follows from Eq. (6) that at  $1 \ll R_\perp \lesssim R_a$  the cross section decreases with  $R_\perp$  relatively slowly,  $\sigma^{\text{DF}} \sim R_\perp^{-2}$ , whereas at  $R_\perp > R_a$  the decrease is already exponential. This means that the projectile is able to efficiently irradiate both atoms of the dimer only provided that the dimer transverse size  $R_\perp$  does not exceed the adiabatic collision radius  $R_a$ . Since  $R_a \sim \gamma v$ , an ultrafast projectile possesses a very large effective interaction range and can probe systems with large dimensions. Simple estimates show that, beginning with impact energies of a few GeV/u, the adiabatic collision radius exceeds the size of the He<sub>2</sub> dimer [5].

The cross section (5) refers to the situation where two helium atoms in the dimer are separated by the vector  $\mathbf{R}$  with the absolute value of its transverse projection  $R_\perp$ . It yields important information about the collisions giving an insight into the basic physics of the fragmentation process [5], but cannot be (directly) measured in the experiment. Therefore, let us ‘‘convert’’ the cross section (5) into quantities which can be measured. We start with the expression

$$\frac{d\sigma_{\text{fr}}^{\text{DF}}}{d^3\mathbf{R}} = \sigma_{A+B^+}^{\text{DF}}(R_\perp) |\Psi_i(\mathbf{R})|^2, \quad (7)$$

where  $\Psi_i(\mathbf{R})$  is the wave function describing the relative motion of the atoms in the ground state of the He<sub>2</sub> dimer.

As was already mentioned, we assume that, before the collision with the projectile, the He<sub>2</sub> dimer was at rest. Let  $\mathbf{P}_A^{\text{rec}}$  and  $\mathbf{P}_B^{\text{rec}}$  be the recoil momenta of the helium ions, which they acquire during the collision because of the interaction with the projectile and electron emission, and let  $\mathbf{P}_A$  and  $\mathbf{P}_B$  be the final momenta of these ions after the Coulomb explosion. Then the energy conservation for the relative motion of the

ionic fragments reads

$$E_K = \frac{\left[\frac{1}{2}(\mathbf{P}_A^{\text{rec}} - \mathbf{P}_B^{\text{rec}})\right]^2}{2\mu} + \frac{Q_A Q_B}{R}. \quad (8)$$

Here,  $E_K = \mathbf{K}^2/(2\mu)$  is the final kinetic energy of the relative motion of the ionic fragments,  $\mathbf{K} = (\mathbf{P}_A - \mathbf{P}_B)/2$  and  $\mu$  are the momentum of their relative motion and the reduced mass, respectively,  $Q_A$  and  $Q_B$  ( $Q_A = Q_B = 1$ ) are their charges and  $R$  is the distance between the ions when the Coulomb explosion began and which, in the case under consideration, coincides with the size of the initial  $\text{He}_2$  dimer at the collision instant. In the energy balance (8) we neglected the kinetic energy of the  $\text{He}^+$  ions, which they had due to the nuclear motion before the collision and which is very small because the depth of the potential well in the  $\text{He}_2$  dimer is just  $\approx 1$  meV.

Since, in the process of single ionization of helium atoms by relativistic projectiles the recoil momenta of the helium ions do not noticeably exceed 1 a.u. [28,29], the first term on the right-hand side of Eq. (8) is in the meV range. Such values are comparable to the Coulomb potential energy  $Q_A Q_B/R$  at the internuclear distances  $R$  of the order of  $10^4$  a.u., which is much larger than the size of the  $\text{He}_2$  (and any known) dimer. Therefore, the neglect of the recoil energy, given by the first term on the right-hand side of Eq. (8), does not have any substantial impact on the energy balance. Thus, the relation

$$E_K = \frac{Q_A Q_B}{R} \quad (9)$$

between the kinetic energy release and the size of the dimer at the collision instant, which neglects the recoil energies, is expected to be very accurate down to energies  $E_K \simeq 10$  meV.

Let us now make a more restrictive assumption that not only the recoil energies are much smaller than the Coulomb energy  $Q_A Q_B/R$  but also that the absolute values of the recoil momenta,  $|\mathbf{P}_A^{\text{rec}}|$  and  $|\mathbf{P}_B^{\text{rec}}|$ , of the fragments are significantly less than  $K = |\mathbf{K}|$ . Since these values do not exceed 1 a.u. the assumption will be fulfilled beginning with  $K \gtrsim 4\text{--}5$  a.u. that corresponds to the energies  $E_K \gtrsim 60$  meV. Under such conditions the momentum  $\mathbf{K}$  will be directed essentially along the internuclear vector  $\mathbf{R}$  of the initial  $\text{He}_2$  dimer and, taking also into account Eq. (9), we obtain

$$d^3\mathbf{R} = \frac{(Q_A Q_B)^3}{\mu K E_K^4} d^3\mathbf{K}. \quad (10)$$

Using Eqs. (7) and Eqs. (9) and (10) we obtain the fragmentation cross section differential in the relative momentum  $\mathbf{K}$  of the ionic fragments

$$\frac{d\sigma_{\text{fr}}^{\text{DF}}}{d^3\mathbf{K}} = \frac{(Q_A Q_B)^3}{\mu K E_K^4} \sigma_{A^+B^+}^{\text{DF}}[R_{\perp}(\mathbf{K})] \times \left| \Psi_i \left( \frac{Q_A Q_B}{E_K} \hat{\mathbf{K}} \right) \right|^2. \quad (11)$$

where  $\hat{\mathbf{K}} = \mathbf{K}/K$ ,  $R_{\perp}(\mathbf{K}) = (Q_A Q_B \sin \Theta_K)/E_K$  and  $\Theta_K$  is the polar angle of the momentum  $\mathbf{K}$  (the  $z$  axis is along the projectile velocity  $\mathbf{v}$ ). Since the bound state of the  $\text{He}_2$  dimer is spherically symmetric, the wave function  $\Psi_i$  does not depend on  $\hat{\mathbf{K}}$ :  $\Psi_i(\frac{Q_A Q_B}{E_K} \hat{\mathbf{K}}) = \Psi_i(\frac{Q_A Q_B}{E_K})$ .

Taking into account that  $d^3\mathbf{K} = K^2 dK d\Omega_K = \mu K dE_K \sin \Theta_K d\mathbf{K} d\varphi_K$ , where  $\varphi_K$  is the azimuthal angle of  $\mathbf{K}$ , and that the right-hand side of Eq. (11) does not depend on  $\varphi_K$  we obtain the fragmentation cross section differential in the kinetic energy release  $E_K$  and the polar angle  $\Theta_K$

$$\frac{d\sigma_{\text{fr}}^{\text{DF}}}{dE_K d\Theta_K} = 2\pi \frac{(Q_A Q_B)^3}{E_K^4} \left| \Psi_i \left( \frac{Q_A Q_B}{E_K} \right) \right|^2 \times \sin \Theta_K \sigma_{A^+B^+}^{\text{DF}}(Q_A Q_B \sin \Theta_K/E_K). \quad (12)$$

In our consideration of the direct fragmentation process, its two steps (“instantaneous” production of two  $\text{He}^+$  ions and the consequent Coulomb explosion of the  $\text{He}^+ \text{--} \text{He}^+$  system) are fully disentangled, even though the energy of the emitted electrons and the kinetic energy release have the same source: the energy transferred by the projectile to the  $\text{He}_2$  dimer. However, since the electrons emitted from helium atoms in collisions with relativistic projectiles have energies extending up to a few tens of eV whereas, as will be seen below, the spectrum of the kinetic energy release in the DF process peaks at  $E_K < 1$  eV and essentially vanishes already at  $E_K \simeq 5\text{--}6$  eV, such a consideration is expected to be quite accurate.

### III. RESULTS AND DISCUSSION

#### A. Preliminary remarks

In this section we report our results for the fragmentation cross sections. In our calculations the ground state of the  $\text{He}_2$  dimer was described by a wave function  $\Psi_i$  corresponding to the dimer binding energy  $I_b$  of 139 neV (this value is very close to that given in [30]): this wave function was used to obtain the results presented below in Figs. 1 to 7. In addition, to explore the sensitivity of the cross sections to the value of  $I_b$ , also wave functions  $\Psi_i$  corresponding to  $I_b = 130$  neV and 148 neV were applied for obtaining the results shown in Fig. 8.

Four different approximations were employed for computing the probabilities  $w$  for single electron removal from a helium atom [see Eq. (4)]. They include (i) the nonrelativistic first Born approximation (nr-FBA); (ii) the nonrelativistic symmetric eikonal approximation (nr-SEA) [31]; (iii) the relativistic first Born approximation (r-FBA); and (iv) the relativistic symmetric eikonal approximation (r-SEA) [29].

The differences between the results obtained by using the first Born and symmetric eikonal approximations offer an idea about the importance of the higher-order effects in the interaction between the projectile and the atoms of the dimer. On the other hand, the differences between results of the relativistic and nonrelativistic approximations yield the information about the role of relativistic effects in the  $\text{He}_2$  fragmentation.

In particular, in the nr-FBA and nr-SEA the speed of light  $c$  is assumed to be infinite, which means that all relativistic effects caused by very high collision velocities vanish. In the r-FBA and r-SEA  $c \approx 137$  a.u. and relativistic effects arising due to high impact energies are taken into account. Since even in very high-energy collisions with helium targets the overwhelming majority of emitted electrons have energies well below 100 eV [32], the main relativistic effects, which are due to high impact energies and which may influence the  $\text{He}_2$  fragmentation, are caused by the deviation of the electric field of the projectile from the (unretarded) Coulomb form.

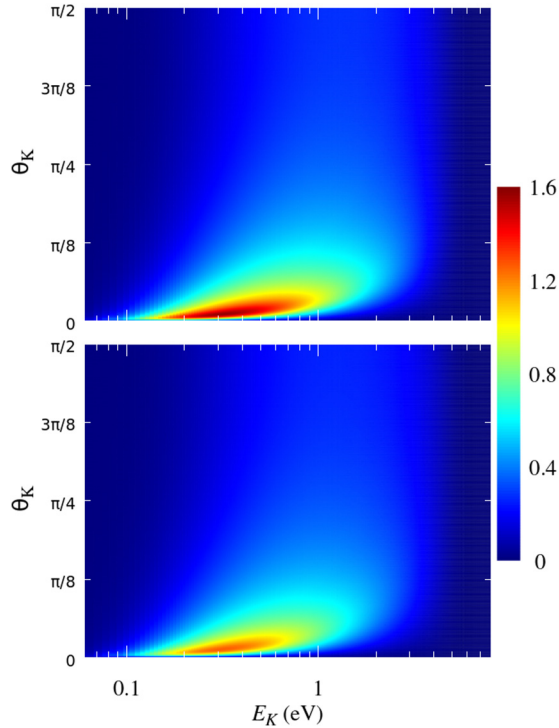


FIG. 1. The cross section  $\frac{d\sigma_{\text{He}}^{\text{DF}}}{dE_K d\Theta_K}$  (in Mb/eV rad) for the fragmentation of the  $\text{He}_2$  dimer by 1 GeV/u  $\text{U}^{92+}$  projectiles given as a function of the kinetic energy release  $E_K$  and the angle  $\Theta_K$ . The upper and lower panels show results obtained using the r-FBA and r-SEA, respectively.

One should say that, in addition to relativistic effects due to high impact velocities, there are also relativistic effects in the ground state of the free  $\text{He}_2$  which, according to the authors of [30], reduce the binding energy of the dimer by about 14%. This affects the form of its wave function (especially at very large internuclear distances) that in turn may have an impact on the shape of the spectrum of the fragments [5].

### B. Fragmentation spectra

In Figs. 1 and 2 we show the doubly differential cross section  $\frac{d\sigma_{\text{He}}^{\text{DF}}}{dE_K d\Theta_K}$  for the fragmentation of the  $\text{He}_2$  dimer into  $\text{He}^+$  ions occurring in collisions with 1 GeV/u and 7 GeV/u  $\text{U}^{92+}$  projectiles, respectively. The corresponding collision velocities and the Lorentz factor are  $v = 120$  a.u.,  $\gamma = 2.08$ , and  $v = 136$  a.u.,  $\gamma = 8.5$ , respectively. The cross section is plotted as a function of the kinetic energy release  $E_K$  and the fragmentation angle  $\Theta_K$  presenting a general picture of the fragmentation spectrum. Taking into account that the spectrum is symmetric with respect to the transformation  $\Theta_K \leftrightarrow \pi - \Theta_K$ , only the interval of angles  $0 \leq \Theta_K \leq \pi/2$  is considered.

It is seen in these figures that the spectrum is predominantly localized in the energy interval  $0.1 \text{ eV} \lesssim E_K \lesssim 2 \text{ eV}$  and at fragmentation angles  $\Theta_K$  not significantly exceeding  $20^\circ$ . It is also seen that at very small energies  $E_K$  the spectrum is restricted to smaller fragmentation angles  $\Theta_K$  whereas with increasing the energy the spectrum shifts to larger  $\Theta_K$ .

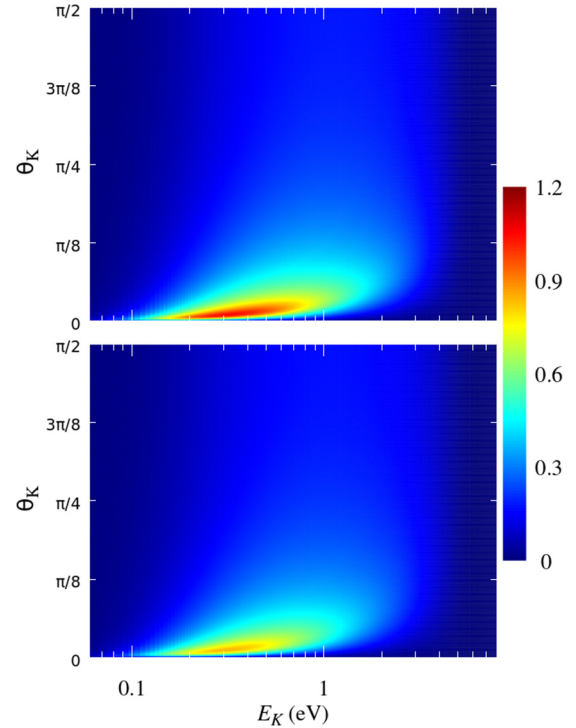


FIG. 2. Same as in Fig. 1 but for the fragmentation by 7 GeV/u  $\text{U}^{92+}$ .

The interval of kinetic energies  $0.1 \text{ eV} \lesssim E_K \lesssim 2 \text{ eV}$  corresponds to the instantaneous size  $R$  of the  $\text{He}_2$  dimer during the collision in the range  $14 \text{ a.u.} \lesssim R \lesssim 270 \text{ a.u.}$  The probability to find the  $\text{He}_2$  dimer in this range is above 90% that is reflected in the dominance of the above energy interval in the spectrum. At energies  $\gtrsim 5\text{--}6 \text{ eV}$  the spectrum practically vanishes since they correspond to the internuclear distances  $R \lesssim 4 \text{ a.u.}$ , where the probability to find the  $\text{He}_2$  dimer is negligibly small.

The cross section  $\sigma_{A^+B^+}^{\text{DF}}$  for the production of two helium ions by the projectile decreases with the transverse size  $R_\perp$  of the dimer at the collision instant ( $\sigma_{A^+B^+}^{\text{DF}} \sim 1/R_\perp^2$  at  $R_\perp < R_d$ ). Since at a fixed  $\Theta_K$  the value of  $R_\perp$  is proportional to  $R$ , the fragmentation with very small  $E_K$  may occur at very small  $\Theta_K$  only, whereas at significantly larger values of  $E_K$  it becomes possible at not very small  $\Theta_K$  as well. Taking also into account that the cross section  $\frac{d\sigma_{\text{He}}^{\text{DF}}}{dE_K d\Theta_K}$  is proportional to the geometrical factor  $\sin \Theta_K$  we can explain the ‘‘shift’’ of the spectrum to larger  $\Theta_K$  with increase in  $E_K$ , which is observed in Figs. 1 and 2.

It also follows from the results presented in Figs. 1 and 2 that, for collisions with so very highly charged projectiles as  $\text{U}^{92}$  ions, the symmetric eikonal approximation predicts a noticeably smaller number of the fragmentation events. This shows that the higher-order effects in the interaction between the projectile and the target remain visible even at very high impact energies. The smaller cross section values, predicted by the symmetric eikonal approximation, reflects the general tendency that in high-energy collisions the higher-order effects reduce cross section values.

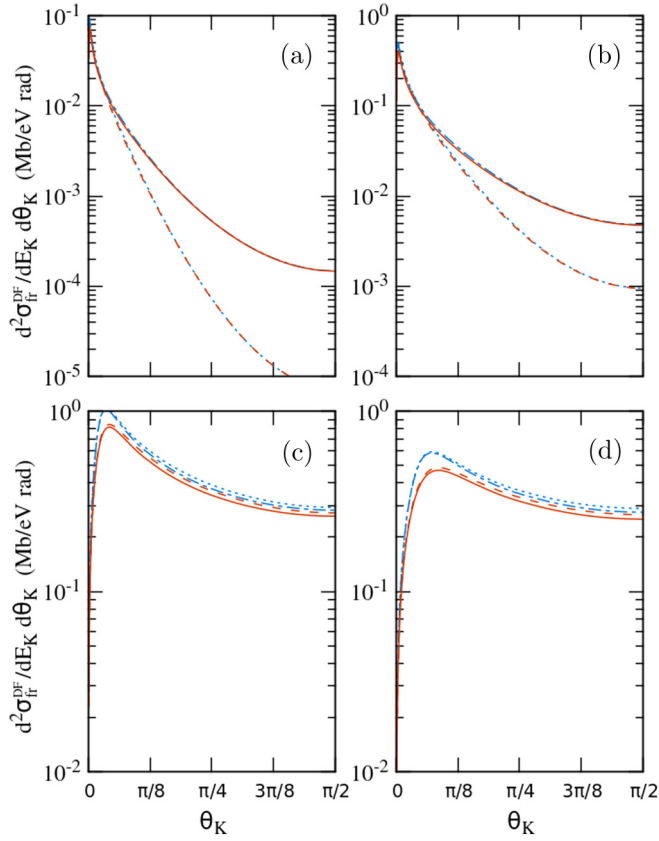


FIG. 3. The cross section  $\frac{d\sigma_{\text{fr}}^{\text{DF}}}{dE_K d\Theta_K}$  for the fragmentation of the  $\text{He}_2$  dimer by 1 GeV/u  $\text{U}^{92+}$  projectiles given as a function of the angle  $\Theta_K$  at fixed values of the energy  $E_K$ : (a) 60 meV, (b) 100 meV, (c) 1 eV, and (d) 2 eV. Dotted, dashed, dash-dotted, and solid curves are results of the calculations in the nr-FBA, the nr-SEA, the r-FBA, and the r-SEA, respectively.

Figures 3 and 4 give more detailed information about the fragmentation process by displaying the cross section  $\frac{d\sigma_{\text{fr}}^{\text{DF}}}{dE_K d\Theta_K}$  as a function of the fragmentation angle  $\Theta_K$  at a given value of the kinetic energy release  $E_K$ : 60 meV, 100 meV, 1 eV, and 2 eV. Some conclusions can be drawn from the results presented in these figures.

First, by comparing the results of the different calculations we see that the shape of the  $\text{He}_2$  fragmentation pattern is in general influenced by both relativistic effects, which arise due to collision velocities approaching the speed of light, and higher-order effects, which originate in a very high charge of the projectile.

Second, the influence of the relativistic effects increases when the kinetic energy release decreases: these effects especially impact the fragmentation events with very small kinetic energy release where they enhance the cross section up to one or two orders of magnitude. On the other hand, the fragmentation with larger values of  $E_K$  is only very modestly influenced by these effects.

Third, the situation with the higher-order effects is just the opposite: their role rises with increasing  $E_K$  and they mostly affect the fragments having larger energies. However, even for such fragments these effects remain modest, reducing the cross-section values not significantly more than 10–20%. The

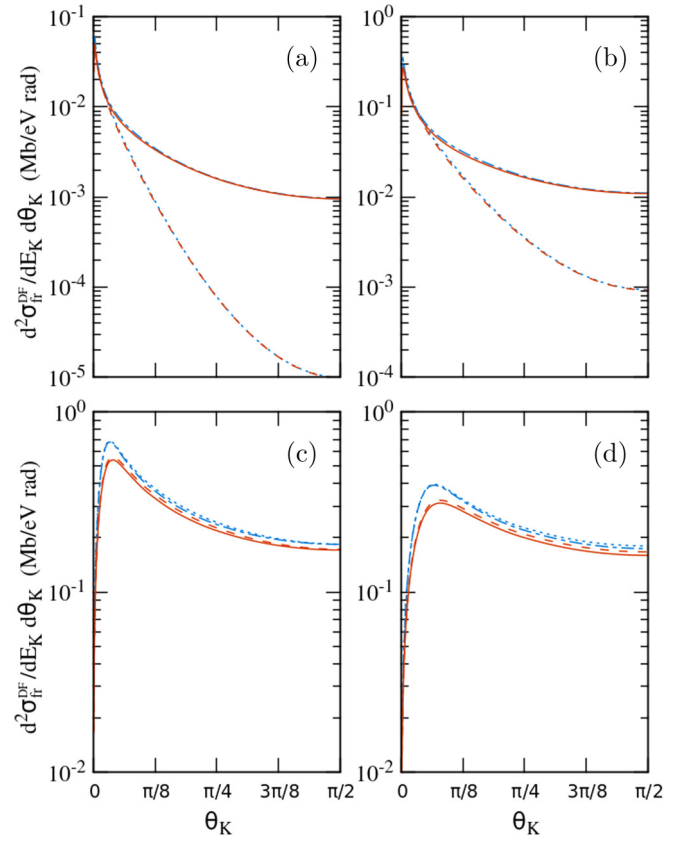


FIG. 4. Same as in Fig. 3 but for collisions with 7 GeV/u  $\text{U}^{92+}$  projectiles.

higher-order effects also somewhat influence the low-energy part of the spectrum: in this case, however, their effect is limited to the very small angles  $\Theta_K$  only.

The above qualitative features of the fragmentation process can be understood by noting that the cross section  $\sigma_{A^+B^+}^{\text{DF}}(R_{\perp})$  is most profoundly influenced by the relativistic effects when the magnitude of  $R_{\perp}$  is large ( $R_a/\gamma < R_{\perp} \lesssim R_a$ ) whereas the higher-order effects are most significant in collisions where the projectile passes close to both atoms of the dimer (the impact parameters  $b$  and  $b'$  do not exceed a few atomic units) that is possible only at relatively small values of  $R_{\perp}$ .

Very large values of  $R_{\perp}$  imply that the instantaneous dimer size  $R$  in the collision has to be very large and, in addition, the dimer orientation angle  $\Theta_R$  should not be small. Since  $E_K = 1/R$  and  $\Theta_R \approx \Theta_K$ , it follows that the relativistic effects are most significant for fragmentation events, which are characterized by a very small kinetic energy release and not too small angles  $\Theta_K$ .

On the other hand, collisions occurring at small values of  $R_{\perp}$ , where the higher-order effects can be substantial, are characterized by either small values of the instantaneous dimer size  $R$  or very small angles  $\Theta_R \approx \Theta_K$  (or a combination of both). The kinetic energy release  $E_K$  of 0.06 eV, 0.1 eV, 1 eV, and 2 eV corresponds to  $R \approx 453$  a.u., 272 a.u., 27.2 a.u., and 13.6 a.u., respectively. To have substantial higher-order effects at the first two values of  $R$  the dimer has to be almost parallel to the collision velocity. As a result, in collisions with very small  $E_K$ , such effects can become visible only at the

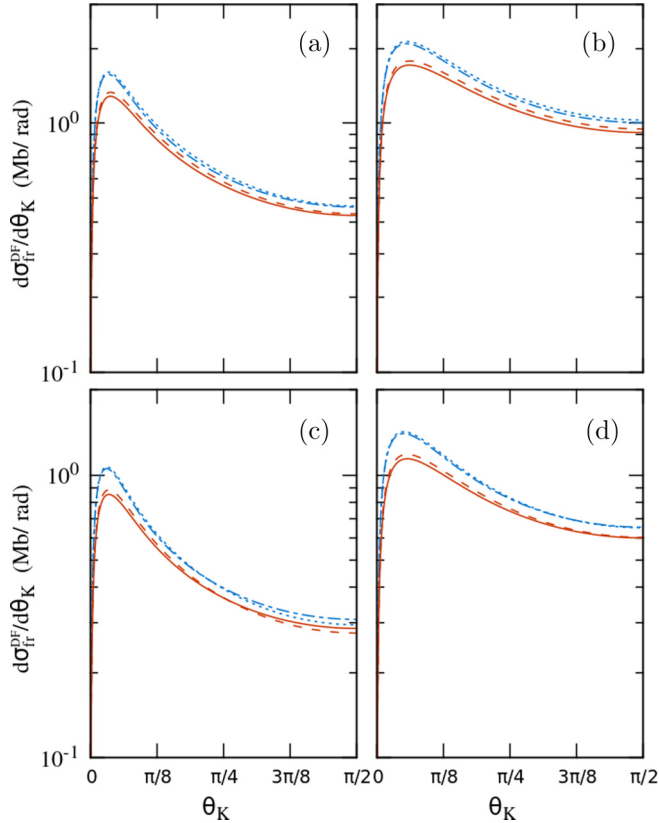


FIG. 5. The angular distribution  $\frac{d\sigma_{\text{fr}}^{\text{DF}}}{d\Theta_K}$  of the  $\text{He}^+$  fragments produced in collisions with 1 GeV/u (two upper panels) and 7 GeV/u (two lower panels)  $\text{U}^{92+}$  projectiles. The results shown in panels (a,c) and (b,d) were obtained by integrating over the energy intervals  $0 \text{ eV} \leq E_K \leq 2 \text{ eV}$  and  $0 \text{ eV} \leq E_K \leq 7 \text{ eV}$ , respectively. Dotted, dash-dotted, dashed, and solid curves represent results of the calculations performed in the nr-FBA, nr-SEA, r-FBA, and r-SEA approximations, respectively.

fragmentation angles  $\Theta_K$  close to zero whose contribution, due to the geometric factor  $\sin \Theta_K$ , is very small. For collisions with larger  $E_K$  the restrictions on the angle  $\Theta_K$  are not so strict and the higher-order effects may be noticeable for the whole range  $0^\circ \leq \Theta_K \leq 90^\circ$ .

The energy  $E_K$  of 0.06 eV, 0.1 eV, 1 eV, and 2 eV correspond to the relative momentum  $K$  of  $\approx 4 \text{ a.u.}$ ,  $5.2 \text{ a.u.}$ ,  $16.4 \text{ a.u.}$ , and  $23.2 \text{ a.u.}$ , respectively. The first two momentum values are not very large. Therefore, in the case of  $E_K = 0.06 \text{ eV}$  and  $0.1 \text{ eV}$  the very narrow peak at very small angles [Figs. 3(a), 3(b), 4(a) and 4(b)] can be noticeably smeared out by the recoil effects.

In Fig. 5 we display the angular distribution of the  $\text{He}^+$  fragments represented by the cross section  $\frac{d\sigma_{\text{fr}}^{\text{DF}}}{d\Theta_K}$ . The cross section was obtained by integrating either over the energy interval  $0 \text{ eV} \leq E_K \leq 2 \text{ eV}$ , in which the direct fragmentation mechanism is by far the dominant one, or over the broader range  $0 \text{ eV} \leq E_K \leq 7 \text{ eV}$ , which covers essentially all energies which are possible in the fragmentation events caused by this mechanism (see Figs. 1 and 2).

Figure 5 shows that the angular distribution of the  $\text{He}^+$  fragments becomes significantly weaker dependent on the angle  $\Theta_K$  when their energy  $E_K$  increases. This feature (which

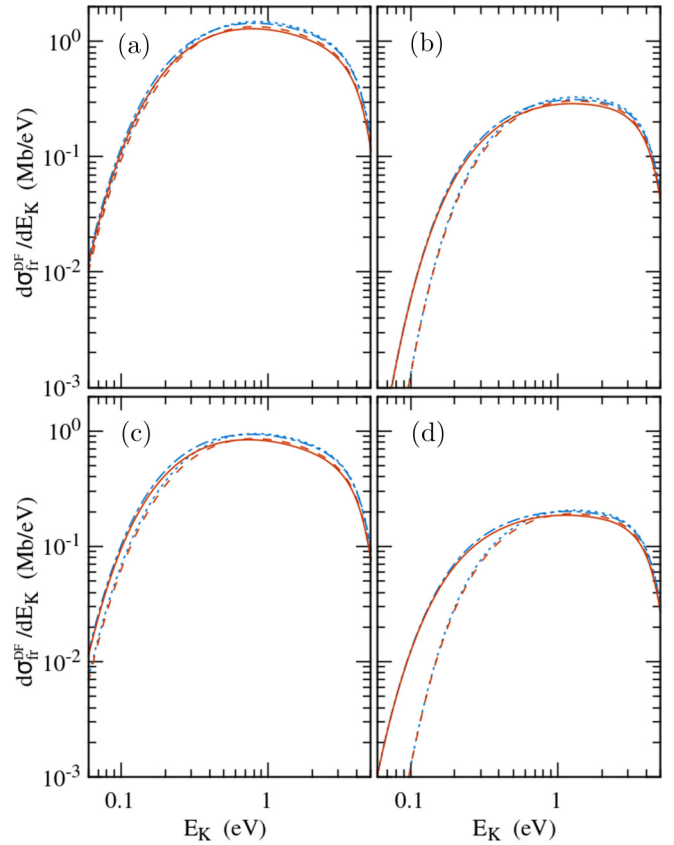


FIG. 6. The energy spectrum  $\frac{d\sigma_{\text{fr}}^{\text{DF}}}{dE_K}$  in the fragmentation of the  $\text{He}_2$  dimer in collisions with 1 GeV/u (the upper panels) and 7 GeV/u (the lower panels)  $\text{U}^{92+}$  projectiles. The results shown in panels (a,c) and (b,d) were obtained by integrating over the angles  $0^\circ \leq \Theta_K \leq 180^\circ$  and  $60^\circ \leq \Theta_K \leq 120^\circ$ , respectively. Dotted, dash-dotted, dashed, and solid curves represent results of the calculations performed in the nr-FBA, nr-SEA, r-FBA, and r-SEA, respectively.

is already seen in Figs. 3 and 4) can be understood by taking into account that, due to the relation  $E_K = 1/R$ , the  $\text{He}^+$  fragments with larger energies emerge when the projectiles hit the  $\text{He}_2$  dimers with smaller size  $R$ . In such collisions the DF mechanism is more efficient causing the  $\text{He}_2$  breakup with significant probabilities even when the dimer is oriented at large angles with respect to the impact velocity.

The energy spectrum  $d\sigma_{\text{fr}}^{\text{DF}}/dE_K$  of  $\text{He}^+$  fragments produced by bombarding the  $\text{He}_2$  dimer by 1 and 7 GeV/u  $\text{U}^{92+}$  projectiles is displayed in Fig. 6. The spectrum shown in the left panels of this figure was obtained by integrating over all possible fragmentation angles,  $0^\circ \leq \Theta_K \leq 180^\circ$ , whereas that given in the right panels includes only the fragments moving at large angles  $60^\circ \leq \Theta_K \leq 120^\circ$ , with respect to the projectile velocity.

The results shown in Fig. 6 confirm the correspondences between the relativistic and higher-order effects and the energy  $E_K$  and angle  $\Theta_K$  of the fragments, which were discussed above. In particular, we again observe that at a given collision velocity the relativistic effects rise when the energy  $E_K$  decreases, becoming especially strong in collisions where the  $\text{He}^+$  fragments possess quite small energies  $E_K$  and move at large angles with respect to the projectile velocity.



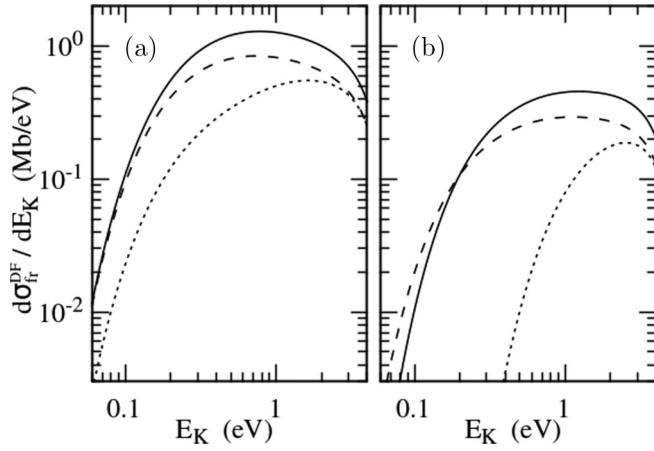


FIG. 7. The energy spectrum  $\frac{d\sigma_{fr}^{DF}}{dE_K}$  for the  $\text{He}_2$  breakup into  $\text{He}^+$  via the DF mechanism calculated within the r-SEA. Results for collisions with 1 GeV/u  $\text{U}^{92+}$ , 7 GeV/u  $\text{U}^{92+}$ , and 11.37 MeV/u  $\text{S}^{14+}$  are shown by solid, dashed, and dotted curves, respectively. The results shown in panels (a) and (b) were obtained by integrating over  $0^\circ \leq \Theta_K \leq 180^\circ$  and  $45^\circ \leq \Theta_K \leq 135^\circ$ , respectively.

In Fig. 7 we compare the energy spectra of the  $\text{He}^+$  ions produced in collisions with 1 and 7 GeV/u  $\text{U}^{92+}$  and 11.37 MeV/u  $\text{S}^{14+}$  ( $v = 21.2$  a.u.,  $\gamma = 1.01$ ). It is seen that the shape of the spectrum profoundly varies with an increase in the impact energy. In particular, the maximum of the energy distribution is shifted from  $E_K \approx 1.7$  eV in collisions with 11.37 MeV/u  $\text{S}^{14+}$  to  $E_K \approx 0.7$  eV in collisions with 7 GeV/u  $\text{U}^{92+}$  where the low-energy part of the spectrum is strongly enhanced [see Fig. 7(a)] and this enhancement becomes even much more pronounced if the fragmentation events with large angles  $\Theta_K$  are selected [Fig. 7(b)].

In collisions with 11.37 MeV/u  $\text{S}^{14+}$  and 7 GeV/u  $\text{U}^{92+}$  the effective strength of the projectile field, given by the ratio  $Z_p/v$ , is essentially the same (0.68 and 0.66, respectively). Therefore, the strong enhancement of the lower-energy part of the fragmentation spectrum, which reflects the corresponding strong increase in the breakup of dimers with very large instantaneous size  $R$ , is caused by a much higher impact energy. One should note, however, that since  $\text{He}_2$  is a very light target, a large increase in the collision velocity has a more profound overall effect on the spectrum shape and the total number of events than an increase in the Lorentz factor  $\gamma$ .

### C. Energy spectrum shape versus the $\text{He}_2$ binding energy

The values for the binding energy  $I_b$  of the  $\text{He}_2$  dimer, reported in the literature, vary between  $I_b = 44.8$  neV [33] and  $I_b = 161.7$  neV [34]. The distribution of the probability density  $\rho(R) = |\Psi_i(R)|^2$  in the ground state of the dimer depends on the value of  $I_b$  and a variation  $\Delta I_b$  in the binding energy would be reflected by the corresponding variation  $\Delta\rho(R)$  of the probability density  $\rho(R)$ . However, if  $\Delta I_b$  is relatively small,  $\Delta I_b \ll I_b$ , a large range of  $R$  has to be spanned in order for the changes in the shape of  $\rho(R)$  to become noticeable.

In this respect, as it was already emphasized in [5], the fragmentation by ultrafast projectiles can be of special inter-

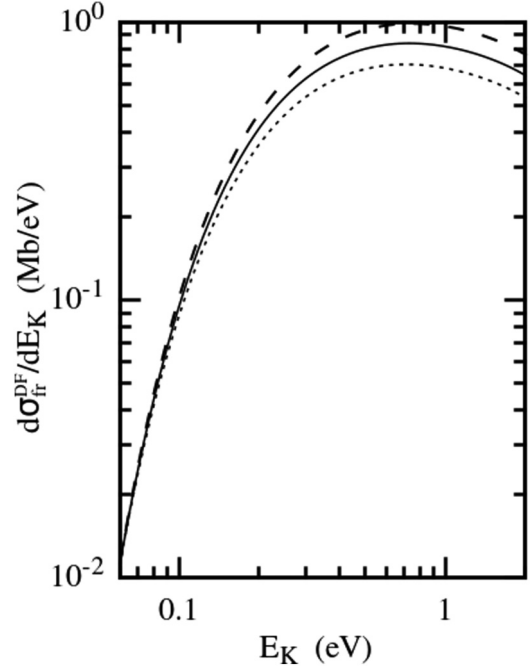


FIG. 8. The cross section  $\frac{d\sigma_{fr}^{DF}}{dE_K}$  versus the binding energy  $I_b$  of the  $\text{He}_2$  in collisions with 7 GeV/u  $\text{U}^{92+}$  projectiles. Solid, dashed, and dotted curves correspond to  $I_b = 139$  neV,  $I_b = 148$  neV, and  $I_b = 130$  neV, respectively. The results for  $I_b = 148$  neV and  $I_b = 130$  neV were normalized to those for  $I_b = 139$  neV at  $E_K = 60$  meV.

est. Indeed, since the adiabatic collision radius  $R_a$  increases with the impact energy as  $\sim v\gamma$ , they possess a very large effective interaction range that is a great advantage in probing the structure of such enormous objects like the  $\text{He}_2$  dimer.

In Fig. 8 we display the energy spectrum  $\frac{d\sigma_{fr}^{DF}}{dE_K}$  for the  $\text{He}_2$  fragmentation by 7 GeV/u  $\text{U}^{92+}$ , calculated using the r-SEA. In the range of  $E_K$ , shown in the figure, the direct fragmentation is by far the dominant breakup channel and the cross section  $\frac{d\sigma_{fr}^{DF}}{dE_K}$  represents the total energy spectrum.

The spectrum was calculated for three values of the dimer binding energy  $I_b$ : 130 neV, 139 neV, and 148 neV. For a better visibility of the variation of the spectrum shape with  $I_b$ , the spectra for  $I_b = 130$  neV and  $I_b = 148$  neV were normalized to the spectrum for  $I_b = 139$  neV at an energy  $E_K = 60$  meV.

In the energy interval,  $60 \text{ meV} \leq E_K \leq 1 \text{ eV}$ , the ratios  $\frac{d\sigma_{fr}^{DF}(I_b=148)/dE_K}{d\sigma_{fr}^{DF}(I_b=139)/dE_K}$ ,  $\frac{d\sigma_{fr}^{DF}(I_b=139)/dE_K}{d\sigma_{fr}^{DF}(I_b=130)/dE_K}$ , and  $\frac{d\sigma_{fr}^{DF}(I_b=148)/dE_K}{d\sigma_{fr}^{DF}(I_b=130)/dE_K}$  vary by about 18%, 20%, and 42%, respectively. The corresponding relative variations,  $\Delta I_b/I_b$ , of the binding energy are approximately 6.5%, 7%, and 14%, respectively. This means that in the energy interval under consideration the shape of the energy spectrum “magnifies” the variation of the binding energy by about three times.

A more detailed analysis of the cross sections shows that the range of quite small  $E_K$  ( $E_K \lesssim 0.2$  eV) gives the main contribution to the variation of the cross section ratios. This is not very surprising since the small energy range,  $60 \text{ meV} \leq E_K \lesssim 0.2$  eV, corresponds to a very large interval, 136 a.u.

$\lesssim R \lesssim 454$  a.u., of the interatomic distances in the  $\text{He}_2$  dimer, where the shape of its ground state becomes sensitive to even a very modest variation of the binding energy. The projectile is able to span in the collision so large an interval of distances since at 7 GeV/u the adiabatic collision radius  $R_a \simeq 10^3$  a.u. already significantly exceeds the size of the dimer.

As it follows from Fig. 8, practically all the variations of the cross section with the binding energy is accumulated in the range  $E_K \leq 0.7$  eV. At so small energies, which correspond to the interatomic distances in the dimer of  $R \geq 39$  a.u., not only the DI-RET mechanism, which is short-ranged, but also the IE-ICD are already fully “turned off” [35,36] and, therefore, have no influence on the shape and the absolute values of the kinetic energy spectra shown in Fig. 8.

#### D. Total fragmentation cross sections

According to our r-SEA calculations, the contribution  $\sigma_{\text{fr}}^{\text{DF}}$  of the DF mechanism to the total cross section for the breakup of the  $\text{He}_2$  dimer in collisions with 1 and 7 GeV/u  $\text{U}^{92+}$  projectiles amounts to 3.65 Mb and 2.4 Mb, respectively.

The relativistic effects in the direct fragmentation are most significant when the “instantaneous” transverse size  $R_{\perp}$  of the  $\text{He}_2$  dimer in the collision is very large. Consequently, they most profoundly influence the fragmentation events with small  $E_K$  and large  $\Theta_K$ . However, such events have relatively small probabilities and, as a result, the cross section  $\sigma_{\text{fr}}^{\text{DF}}$  is very weakly influenced by the relativistic effects. In particular, for collisions with 1 and 7 GeV/u  $\text{U}^{92+}$  the difference between our results for  $\sigma_{\text{fr}}^{\text{DF}}$ , obtained using relativistic and nonrelativistic approaches, is about merely  $\simeq 1\%$ .

The field of the projectile acting on the dimer is strongest when the impact parameters with respect to both atomic sites of the dimer are small, i.e., in collisions where the “instantaneous” transverse size  $R_{\perp}$  of the dimer is not large. Since such collisions give a more significant contribution to  $\sigma_{\text{fr}}^{\text{DF}}$  than those with very large  $R_{\perp}$ , the influence of the higher-order effects in the interaction between the projectile and the dimer on the magnitude of  $\sigma_{\text{fr}}^{\text{DF}}$  is substantially larger, reaching about 14% for the fragmentation by 1 and 7 GeV/u  $\text{U}^{92+}$ .

In the present paper the  $\text{He}_2$  fragmentation via the IE-ICD and DI-RET mechanisms was not calculated. Nevertheless, we can still obtain a rough estimate for the contribution to the total fragmentation cross section due to these two mechanisms. According to the experimental results of [3], in the breakup of the  $\text{He}_2$  dimer by 11.37 MeV/u  $\text{S}^{14+}$  the ratio of the summed contributions of the IE-ICD and DI-RET channels to the contribution of the DF channel is approximately equal to 1.6. Taking into account that our calculation for the DF contribution in collisions with 11.37 MeV/u  $\text{S}^{14+}$  yields 1.8 Mb, we obtain that the summed contributions of the IE-ICD and DI-RET to the fragmentation by 11.37 MeV/u  $\text{S}^{14+}$  is  $\approx 1.8 \times 1.6 = 2.9$  Mb.

The cross sections for the fragmentation via the IE-ICD and DI-RET are proportional to the cross sections for simultaneous ionization-excitation and double ionization, respectively, of the helium atom. Both these cross sections scale similarly with  $Z_p$  and  $v$ . Therefore, by calculating them for collisions with 11.37 MeV/u  $\text{S}^{14+}$  and 1 and 7 GeV/u  $\text{U}^{92+}$  projectiles, we estimated that the summed contribution of

the IE-ICD and DI-RET mechanisms to the fragmentation in collisions with 1 and 7 GeV/u  $\text{U}^{92+}$  is roughly equal to 4.3 Mb and 3 Mb, respectively.

#### IV. CONCLUSION

In conclusion, we studied the fragmentation of the helium dimer into singly charged helium ions by relativistic highly charged projectiles in collisions with relatively low kinetic energy release  $E_K \lesssim 3\text{--}4$  eV. Such breakup events occur solely due to the direct fragmentation mechanism in which the projectile ionized both dimer’s atoms in a single collision. In this mechanism the two helium ions are produced within the so short time interval ( $\lesssim 10^{-16}$  s) that during the production the helium nuclei remain essentially at rest. Consequently, the energy  $E_K$  of the ionic fragments, produced via the direct mechanism, is very simply ( $E_K = 1/R$ ) related to the size  $R$  of the  $\text{He}_2$  dimer at the collision instant.

We investigated in detail the energy and angular spectra of the  $\text{He}^+$  ions produced in collisions with 1 and 7 GeV/u  $\text{U}^{92+}$  projectiles. Our main findings can be summarized as follows.

In collisions with  $\gamma \gg 1$  the fragmentation events, in which the  $\text{He}^+$  ions move with low kinetic energies ( $E_K \lesssim 0.1$  eV or  $E_K \ll 1$  eV) under large angles ( $20^\circ \lesssim \Theta_K \lesssim 160^\circ$ ) with respect to the projectile velocity are strongly affected by the relativistic effects.

The shape of the energy spectrum of the  $\text{He}^+$  ions is quite sensitive to the binding energy of the  $\text{He}_2$  dimer, which can be exploited for its precise determination. Here the relativistic effects also play an important role since, by significantly enhancing the lower-energy part of the spectrum, they enable one to span a substantially broader range of the interatomic distances  $R$  in the dimer, effectively increasing the sensitivity of the spectrum shape to the variation of the dimer binding energy.

The relativistic effects, having a strong impact on the fragments with low  $E_K$  and large  $\Theta_K$  and making the energy spectrum shape more sensitive to the variation in the dimer binding energy, nevertheless very weakly influence the total amount of the fragmentation events caused by the direct mechanism because they affect only their minor part. In this respect, a large increase in the collision velocity has a much stronger overall effect on the spectrum shape and the total number of events.

In contrast to relativistic effects, the role of the higher-order effects in the projectile-dimer interaction rises with increasing energy of the  $\text{He}^+$  fragments becoming substantial at  $E_K \gtrsim 1$  eV. Since such events give a more significant contribution to the fragmentation than those with very small  $E_K$ , the influence of the higher-order effects is substantially larger reaching about 14% for the total cross section in the direct fragmentation by 1 and 7 GeV/u  $\text{U}^{92+}$ .

According to our calculations the contribution of the direct mechanism to the total cross section for the  $\text{He}_2$  fragmentation by 1 and 7 GeV/u  $\text{U}^{92+}$  amounts to 3.65 Mb and 2.4 Mb, respectively. A rough estimate for the total fragmentation cross section in these collisions, which takes into account all the fragmentation mechanisms, suggests that it is about two times larger than the above values.

## ACKNOWLEDGMENTS

BN, SFZ, and XM gratefully acknowledge the support from the National Key Research and Development Program of China (Grant No. 2017YFA0402300) and the CAS President's

Fellowship Initiative. Our numerical results were obtained using the facilities of the Supercomputer Center HIRFL at the Institute of Modern Physics of Chinese Academy of Sciences (Lanzhou, China).

- [1] J. Titze, M. S. Schöffler, H.-K. Kim, F. Trinter, M. Waitz, J. Voigtsberger, N. Neumann, B. Ulrich, K. Kreidi, R. Wallauer *et al.*, *Phys. Rev. Lett.* **106**, 033201 (2011).
- [2] H.-K. Kim, H. Gassert, J. N. Titze, M. Waitz, J. Voigtsberger, F. Trinter, J. Becht, A. Kalinin, N. Neumann, C. Zhou *et al.*, *Phys. Rev. A* **89**, 022704 (2014).
- [3] H.-K. Kim, Ph.D. Thesis, Frankfurt University, 2014.
- [4] A. Jacob, C. Müller, and A. B. Voitkiv, *Phys. Rev. A* **103**, 042804 (2021).
- [5] B. Najjari, Z. Wang, and A. B. Voitkiv, *Phys. Rev. Lett.* **127**, 203401 (2021).
- [6] R. E. Grisenti, W. Schöllkopf, J. P. Toennies, G. C. Hegerfeldt, T. Köhler, and M. Stoll, *Phys. Rev. Lett.* **85**, 2284 (2000).
- [7] B. A. Friedrich, *Physics* **6**, 42 (2013).
- [8] H. B. G. Casimir and D. Polder, *Phys. Rev.* **73**, 360 (1948).
- [9] F. Luo, G. Kim, G. C. McBane, C. F. Giese, and W. R. Gentry, *J. Chem. Phys.* **98**, 9687 (1993); M. Jeziorska, W. Cencek, K. Patkowski, B. Jeziorski, and K. Szalewicz, *ibid.* **127**, 124303 (2007).
- [10] T. Havermeier, T. Jahnke, K. Kreidi, R. Wallauer, S. Voss, M. Schöffler, S. Schossler, L. Foucar, N. Neumann, J. Titze *et al.*, *Phys. Rev. Lett.* **104**, 153401 (2010).
- [11] T. Havermeier, T. Jahnke, K. Kreidi, R. Wallauer, S. Voss, M. Schöffler, S. Schossler, L. Foucar, N. Neumann, J. Titze *et al.*, *Phys. Rev. Lett.* **104**, 133401 (2010).
- [12] N. Sisourat, N. V. Kryzhevoi, P. Kolorenc, S. Scheit, T. Jahnke, and L. S. Cederbaum, *Nat. Phys.* **6**, 508 (2010).
- [13] S. Zeller, M. Kunitski, J. Voigtsberger *et al.*, *Proc. Natl. Acad. Sci. USA* **113**, 14651 (2016).
- [14] For example, in collisions of 1 GeV/u  $\text{U}^{92+}$  with He the radiative electron capture cross section  $\sigma_{\text{rec}} \simeq 10^{-23} \text{ cm}^2$  (see, e.g., results for radiative recombination on p. 272 of [15]) is about eight orders of magnitude smaller than the cross section for the single ionization of He  $\sigma_i \approx 10^{-15} \text{ cm}^2$  (see, e.g., [17]). The process of nonradiative electron capture is characterized by even much weaker cross sections.
- [15] J. Eichler and W. E. Meyerhof, *Relativistic Atomic Collisions* (Academic Press, San Diego, CA, 1995).
- [16] A. B. Voitkiv and A. V. Koval, *J. Phys. B: At. Mol. Opt. Phys.* **31**, 499 (1998).
- [17] A. B. Voitkiv, B. Najjari, R. Moshhammer, and J. Ullrich, *Phys. Rev. A* **65**, 032707 (2002).
- [18] B. Najjari and A. B. Voitkiv, *Phys. Rev. A* **104**, 033104 (2021).
- [19] J. Matthew and Y. Komninos, *Surf. Sci.* **53**, 716 (1975).
- [20] For example,  $\alpha = 3/(8\pi)$  and  $3/(2\pi)$  for the  $2p_{\pm 1} \rightarrow 1s$  and  $2p_0 \rightarrow 1s$  transitions in  $\text{He}^+$ , respectively, see, e.g., F. Grüll, A. B. Voitkiv, and C. Müller, *Phys. Rev. Research* **2**, 033303 (2020).
- [21] L. S. Cederbaum, J. Zobeley, and F. Tarantelli, *Phys. Rev. Lett.* **79**, 4778 (1997); R. Santra, J. Zobeley, L. S. Cederbaum, and N. Moiseyev, *ibid.* **85**, 4490 (2000).
- [22] This mechanism was initially considered in [2] for collisions of 11.37 MeV/u  $\text{S}^{14+}$  with  $\text{He}_2$  dimers having the “instantaneous” internuclear distance  $R$  in the range  $5 \text{ a.u.} \leq R \leq 10 \text{ a.u.}$
- [23] For the  $\text{He}_2$  fragmentation by photo absorption a similar mechanism was explored experimentally and theoretically in [10] and [18], respectively.
- [24] In [5] the probabilities  $P_{A^+}(\mathbf{b})$  and  $P_{B^+}(\mathbf{b}')$  were defined as  $P_{A^+}(\mathbf{b}) = 2w(\mathbf{b})$  and  $P_{B^+}(\mathbf{b}') = 2w(\mathbf{b}')$ . The inclusion of the factors  $[1 - w(\mathbf{b})]$  and  $[1 - w(\mathbf{b}')$ ] somewhat reduces the cross-section values compared to those reported in [5].
- [25] F. Martín and A. Salin, *Phys. Rev. A* **55**, 2004 (1997).
- [26] M. Abramowitz and I. Stegun, *Handbook of Mathematical Functions* (Dover, New York, 1964).
- [27] For instance, in the interval  $50 \text{ a.u.} \lesssim R_{\perp} \lesssim 500 \text{ a.u.}$  the value of  $C$  varies by just about 16% (between 0.56 and 0.65 if  $R_{\perp}$ ,  $R_a$ ,  $Z_p$ , and  $v$  are given in a.u. while the cross section is in Mb).
- [28] R. Moshhammer, W. Schmitt, J. Ullrich, H. Kollmus, A. Cassimi, R. Dorner, O. Jagutzki, R. Mann, R. E. Olson, H. T. Prinz, Schmidt-H. Bocking, and L. Spielberger, *Phys. Rev. Lett.* **79**, 3621 (1997).
- [29] A. B. Voitkiv and B. Najjari, *J. Phys. B: At. Mol. Opt. Phys.* **37**, 4831 (2004).
- [30] M. Przybytek, W. Cencek, J. Komasa, G. Lach, B. Jeziorski, and K. Szalewicz, *Phys. Rev. Lett.* **104**, 183003 (2010).
- [31] P. D. Fainstein and R. D. Rivarola, *J. Phys. B* **20**, 1285 (1987).
- [32] A. B. Voitkiv, B. Najjari, and J. Ullrich, *J. Phys. B: At. Mol. Opt. Phys.* **38**, L107 (2005).
- [33] R. Feltgen, H. Kirst, K. A. Köhler *et al.*, *J. Chem. Phys.* **76**, 2360 (1982).
- [34] A. R. Janzen and R. A. Aziz, *J. Chem. Phys.* **107**, 914 (1997).
- [35] According to the results of [11] and [12] on the  $\text{He}_2$  photo fragmentation proceeding via ICD, the range  $E_K \leq 2 \text{ eV}$  yields a negligibly small contribution to this process.
- [36] Our rough estimates for the contribution of the DI-RET mechanism suggest that at  $E_K \leq 1 \text{ eV}$  it is about four orders of magnitude smaller than that of the DF.